

Lithium depletion in solar-like stars: no planet connection

P. Baumann¹, I. Ramírez¹, J. Meléndez², M. Asplund¹, and K. Lind³

¹ Max Planck Institute for Astrophysics, Postfach 1317, 85741 Garching, Germany
e-mail: [pbaumann, ivan, asplund]@mpa-garching.mpg.de

² Centro de Astrofísica da Universidade do Porto, Rua das Estrelas, 4150-762 Porto, Portugal
e-mail: jorge@astro.up.pt

³ European Southern Observatory (ESO), Karl-Schwarzschild-Str. 2, 85748 Garching, Germany
e-mail: klind@eso.org

Received 2 June 2010 / Accepted 24 June 2010

ABSTRACT

We have determined precise stellar parameters and lithium abundances in a sample of 117 stars with basic properties very similar to the Sun. This sample selection reduces biasing effects and systematic errors in the analysis. We estimate the ages of our sample stars mainly from isochrone fitting but also from measurements of rotation period and X-ray luminosity and test the connection between lithium abundance, age, and stellar parameters. We find strong evidence for increasing lithium depletion with age. Our sample includes 14 stars that are known to host planets and it does not support recent claims that planet-host stars have experienced more lithium depletion than stars without planets. We find the solar lithium abundance normal for a star of its age, mass, and metallicity. Furthermore, we analyze published data for 82 stars that were reported to support an enhanced lithium depletion in planet hosts. We show that those stars in fact follow an age trend very similar to that found with our sample and that the presence of giant planets is not related to low lithium abundances. Finally, we discuss the systematic biases that led to the incorrect conclusion of an enhanced lithium depletion in planet-host stars.

Key words. Sun: abundances – stars: abundances – planetary systems

1. Introduction

The lithium abundances of solar-like stars in the solar neighborhood spread over more than two orders of magnitude, which is much larger than the range of abundances seen for other elements (e.g., Reddy et al. 2003). The Sun, in particular, has a very low lithium abundance compared to many nearby solar analogs (e.g., Lambert & Reddy 2004). Furthermore, the photospheric solar lithium abundance is about 160 times lower than that measured in meteorites ($\log \epsilon_{\text{Li},\odot} = 1.05 \pm 0.10 \text{ dex}^1$, $\log \epsilon_{\text{Li,met}} = 3.26 \pm 0.05 \text{ dex}$; both values are from Asplund et al. 2009). This difference between the current solar and protosolar values is not predicted by standard stellar evolution models (e.g., D’Antona & Mazzitelli 1984).

The wide range of observed lithium abundances in nearby solar-like stars is most likely due to a dependency between $\log \epsilon_{\text{Li}}$ and the star’s age and mass (e.g., Montalbán & Schatzman 2000; Charbonnel & Talon 2005; Xiong & Deng 2009; Do Nascimento et al. 2009). Lithium is easily destroyed by proton capture reactions in stellar interiors. Thus, if lithium is transported between the chemically mixed outer convection zone and deeper lying regions with temperatures that are high enough for lithium destruction, the photospheric abundance will decrease with time. Macroscopic transport processes in the radiative zone below the convective envelope contribute to the lowering of the surface lithium abundance throughout the main-sequence stage. This would explain why the photospheric solar abundance is

much smaller than the meteoritic one. We expect an enhanced lithium depletion in stars with larger convection zones on the main sequence as well as in stars with a higher degree of differential rotation between the radiative core and the convective envelope (see below). The reason is that lithium is only depleted as it moves to deeper and therefore hotter regions of a star, where the temperature is high enough (about 2.5 million K) for proton capture (see, e.g., Pinsonneault 1997).

Recently, it has been suggested that the presence of planets around a star could affect the evolution of the photospheric lithium abundance (e.g., Bouvier 2008). A long-lasting star-disk interaction during the star’s pre-main sequence phase could slow down the host-star’s rotation and therefore increase the degree of differential rotation between the star’s core and envelope. Rotationally-driven mixing is then enhanced, thus destroying more lithium than in stars without planets because fast rotators evolve with little core-envelope decoupling. Planet migration affects the star’s angular momentum, which might also have an impact on $\log \epsilon_{\text{Li}}$. Finally, the ingestion of a planet can increase the surface lithium abundance (e.g., Montalbán & Rebolo 2002; Israelian et al. 2001).

The possibility of a lithium-planet connection is subject of ongoing discussions. Recent work by Gonzalez (2008), Gonzalez et al. (2010), Castro et al. (2008), and Israelian et al. (2009) suggests a possible $\log \epsilon_{\text{Li}}$ -planet dependency, whereas Ryan (2000) and Luck & Heiter (2006) find that stars with planets show the same lithium distribution as the comparison field stars. Takeda et al. (2007, 2010) describe the stellar angular momentum as the crucial factor that determines the lithium abundance of solar-like stars and find that slow rotators show an enhanced lithium depletion. Planets *could* be the reason for a slow

¹ We use the standard notation $\log \epsilon_X = \log \frac{n_X}{n_H} + 12$, where n_X and n_H are the the number densities of element X and hydrogen, respectively. Also, for metallicities we use the common abbreviation $[\text{Fe}/\text{H}] = \log \epsilon_{\text{Fe}} - \log \epsilon_{\text{Fe},\odot}$.

rotation, but they were not able to draw firm conclusions due to the low number of planet hosts in their sample and the fact that their use of the star's projected rotational velocity, $v \sin i$, instead of measured rotation periods introduces additional uncertainty, since the inclination angle i is unknown.

From a practical point of view, an enhanced lithium depletion in planet-hosts would be greatly beneficial for the search for extrasolar planets, because all known methods for extrasolar planet detection (e.g., radial velocity, transits, or microlensing) are very time consuming. With an enhanced lithium depletion, however, one could preselect planet-host candidates just by obtaining the stars' chemical composition.

In this paper, we derive lithium abundances and ages for a sample of solar-type stars to examine whether there is a correlation between lithium and age as well as a possible connection between lithium and planets. We also examine lithium abundances and ages for the solar analog sample of [Israeli et al. \(2009\)](#), who claim to have found evidence for an enhanced lithium depletion in planet-host stars.

2. Observations and analysis

Our sample consists of 117 solar-like stars selected from the Hipparcos catalog ([Perryman et al. 1997](#)) as in [Meléndez & Ramírez \(2007\)](#). They were observed at the McDonald (Robert G. Tull coudé spectrograph on the 2.7 m Harlan Smith telescope; RGT), Las Campanas (MIKE spectrograph on the 6.5 m Magellan Clay telescope), and La Silla (HARPS spectrograph on the 3.6 m ESO telescope) observatories. Our few solar twins observed at Keck ([Meléndez et al. 2006](#)) are not discussed here since they are already included in the McDonald sample.

The RGT and MIKE data (spectra as well as stellar parameters) are from [Ramírez et al. \(2009\)](#), hereafter R09) and [Meléndez et al. \(2009, 2010\)](#), hereafter M09), respectively; two stars (HIP 10215 and HIP 79672) are part of both samples. HARPS spectra for 12 more stars were obtained from the ESO archive, while spectra for 6 other stars were obtained from the S⁴N database ([Allende Prieto et al. 2004](#))². One of the objects (HIP 80337) occurs in both the HARPS and the S⁴N samples (we use the HARPS parameters, because they have the smaller uncertainties), so that we have 17 additional stars. The spectra for these stars were analyzed in an identical fashion as in R09 (see below). All sub-samples contain one or more solar reference objects for normalization: R09 used the light reflected from the asteroids Ceres and Vesta, M09 used Vesta, and for the stars added in this work, spectra of asteroid Ceres, Jupiter's moon Ganymedes, and the Moon were used. Table 1 shows the specifications of each sub-sample, where the last two lines describe the additional data from this work. All spectra have a signal-to-noise ratio (S/N) greater than about 200, which allows the determination of lithium abundances as low as solar. Note that three stars in our sample are also included in M09 (HIP 79672) and R09 (HIP 14614 and HIP 42438). For the further analysis, we use the parameters with the smaller uncertainties.

The HARPS and S⁴N data were analyzed by first measuring Fe I and Fe II equivalent widths (EWs), where a line list of 45 iron lines (34 Fe I and 11 Fe II lines) within the wavelength range from 4445 to 8294 Å was used. The Fe lines have a broad range of excitation potentials (from ~0.1 to ~4.6 eV). The line list adopted is from Scott et al. (in prep.; see also

Table 1. Specifications for the different sub-samples.

Sample name	Instrument/telescope	Wavelength coverage (in Å)	Spectral resolution $R = \Delta\lambda/\lambda$	Number of stars
R09	RGT/McDonald	3800–9125	60 000	63
M09	MIKE/Magellan	3400–10 000	65 000	42
this work	RGT/McDonald, HARPS/ESO	3800–9125, 3783–6865	45 000–110 000	18

[Asplund et al. 2009](#)). To calculate the iron abundances ([Fe/H]) from the Fe I/Fe II lines, we used the spectrum synthesis program *MOOG* ([Snedden 1973](#)) and ATLAS 9 model atmospheres without convective overshoot (e.g., [Kurucz 1993](#)). We iteratively assigned the stellar parameters effective temperature, surface gravity, and microturbulent velocity by forcing simultaneously Fe I excitation equilibrium and Fe I/Fe II ionization equilibrium. For a more detailed description see [Ramírez et al. \(2009\)](#). With the method described above, we derived the following mean errors: $\sigma(T_{\text{eff}}) = 40$ K, $\sigma(\log g) = 0.06$ dex, and $\sigma([\text{Fe}/\text{H}]) = 0.025$ dex.

Stellar ages and masses were determined primarily from the location of stars on the theoretical HR-diagram (T_{eff} vs. $\log g$) as compared to theoretical predictions based on stellar evolution calculations (isochrones). We produced a grid of Y^2 isochrones (e.g., [Yi et al. 2001](#)) with steps of 0.01 dex in metallicity around the solar value. For each star, we computed the age probability distribution of all isochrone points included within a $3\text{-}\sigma$ radius from the observed stellar parameters. The adopted mean age and $1\text{-}\sigma$ Gaussian-like upper and lower limits were derived from the age probability distribution (e.g., [Lachaume et al. 1999](#); [Reddy et al. 2003](#)). Although isochrone ages of unevolved stars are typically unreliable, the high precision of our stellar parameters allowed us to infer reasonably accurate absolute isochrone ages, even for stars as young as ~3 Gyr; relative ages are naturally even better determined. For most stars younger than about 3 Gyr only upper limits could be determined. For these younger stars, we adopted ages based on measurements of rotational periods ([Gaidos et al. 2000](#); [Barnes 2007](#)) and X-ray luminosity ([Agüeros et al. 2009](#)) along with the rotation-age relation by [Barnes \(2007\)](#) and the X-ray luminosity-age relation by [Guinan & Engle \(2009\)](#). In a few cases of stars in the intermediate age region (2–4 Gyr), an average of isochrone and rotational ages was determined to improve the age estimate. For stars with very unreliable isochrone ages we used the activity-based ages by [Mamajek & Hillenbrand \(2008\)](#) and [Saffe et al. \(2005\)](#). Our adopted ages and the methods to obtain them are listed in Table 4.

Using our stellar parameters as well as those in R09 and M09, we derived the lithium abundances for all 117 stars with line synthesis using *MOOG*. For this purpose we generated a line list from 6697 to 6717 Å, i.e. 10 Å around the lithium doublet at 6707.8 Å. The whole wavelength range was synthesized with *MOOG*, where hyperfine splitting and the Li-doublet were taken into account. Knowing the basic stellar parameters, we were able to fit the lithium line including the effects of the projected rotational velocity $v \sin i$ and the microturbulent and macroturbulent velocities. We derived lithium abundances with a mean error of $\sigma = 0.05$ dex for stars in which the lithium doublet was detected. Our mean of all solar spectra is $\log \epsilon_{\text{Li}} = 1.03 \pm 0.04$ dex.

Initially, we derived Li abundances assuming line formation in LTE (local thermal equilibrium), in 1D, hydrostatic, plane parallel ATLAS 9 model atmospheres. Abundance corrections were

² The Spectroscopic Survey of Stars in the Solar Neighbourhood (S⁴N) data and more detailed information can be found at <http://hebe.as.utexas.edu/s4n/>

Table 2. Age and lithium abundance of solar twins in open clusters of near solar metallicity.

Cluster	Age in Gyr	$\log \epsilon_{\text{Li}}$	$\sigma(\log \epsilon_{\text{Li}})$	[Fe/H]	Source
IC 2602 & IC 2391	0.030	2.9	0.1	-0.05	Randich et al. (2001)
Pleiades	0.07	2.8	0.1	-0.03	Soderblom et al. (1993)
Blanco 1	0.10	2.9	0.1	+0.04	Ford et al. (2005)
M 34 (NGC 1039)	0.25	2.8	0.1	+0.07	Jones et al. (1997)
Coma Berenices	0.6	2.4	0.15	-0.05	Ford et al. (2001)
NGC 762	2.0	2.1	0.1	+0.01	Sestito et al. (2004)
M 67	3.9	1.2	0.5	+0.05	Pasquini et al. (2008)

Notes. Data are from the compilation by Sestito & Randich (2005).

thereafter applied to account for departures from LTE in the formation of the Li resonance line. The non-LTE modeling procedure is the same as described in Lind et al. (2009), but extended to cover also super-solar metallicities. For our sample stars, the abundance corrections range from -0.03 dex to $+0.08$ dex, depending on the lithium line strength and exact stellar parameters. In stars for which the equivalent width of the lithium line is below ~ 100 mÅ, over-ionization of neutral lithium results in positive abundance corrections, increasing with increasing metallicity and decreasing effective temperature. When the line starts to become saturated, increased photon losses pushes the statistical equilibrium in the opposite direction, i.e. into over-recombination, resulting in negative corrections for some stars (see Lind et al. 2009, for more details). The non-LTE corrections are very small in comparison to the full range covered in lithium abundance, and hence the qualitative results of this study are the same for lithium abundances inferred in LTE and non-LTE. Note that the NLTE corrections are computed using MARCS models (Gustafsson et al. 2008). Our NLTE corrected solar lithium abundance is 1.07 ± 0.04 , in good agreement with the 3D-NLTE estimate by Asplund et al. (2009).

Our adopted stellar parameters and derived LTE and non-LTE lithium abundances are given in Table 4. Figure 1 shows the good agreement between the three observational sub-samples, which reduces errors introduced by inhomogeneous data processing and therefore makes the analysis more reliable. It also is a proof of the consistently good quality of the data.

We have also considered the lithium abundances of solar twins from 8 open clusters as listed in Table 2. Data are from the compilation by Sestito & Randich (2005) as shown in Table 2 with updated data for M 67 by Pasquini et al. (2008). The age for M 67 is taken from Vandenberg et al. (2007) and Yadav et al. (2008), the lithium abundances for M 67 stars are from Castro et al. (2010). The clusters IC 2602 and IC 2391 are listed as one here, because their parameters are basically the same. We only used open clusters around solar metallicity (0.0 ± 0.1 dex) and with reliable data. The solar twins that we select in open clusters are stars of one solar mass by definition, i.e. they are main sequence stars with $1 M_{\odot}$ based on their effective temperature. We take into account the increase of the solar effective temperature with increasing age in the selection of stars from open clusters.

3. Results

3.1. Lithium and age

Using our sample of solar-like stars a clear lithium-age trend is observed (Fig. 2). The dependency is as expected: older stars show more lithium depletion. The Spearman correlation coefficient is $r_{\text{tot}} = -0.61$. This trend becomes clearer when we restrict the sample to solar twins, as in Fig. 3. We define solar twins as

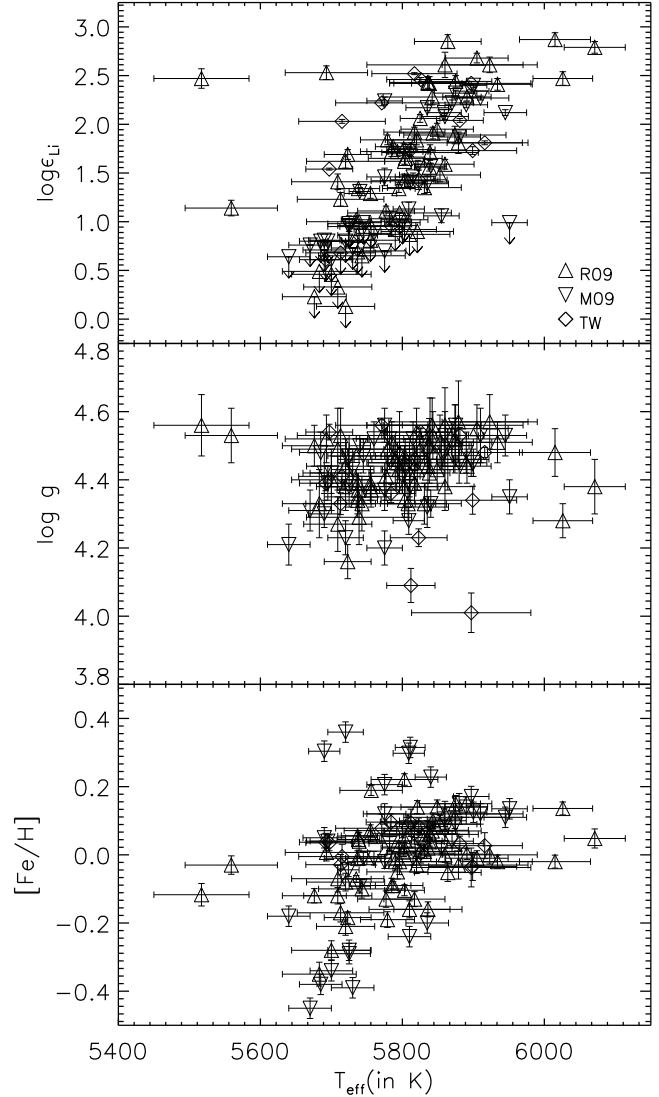


Fig. 1. NLTE lithium abundance, $\log g$, and metallicity plotted against effective temperature. R09 and M09 stand for data from Ramírez et al. (2009) and Meléndez et al. (2009, 2010), respectively; TW is data re-analyzed in this work.

stars with $[\text{Fe}/\text{H}] = 0.0 \pm 0.1$ and $M = (1.00 \pm 0.04) M_{\odot}$. The stars from the open clusters given in Table 2 fit the trend in Fig. 3 very well. This is very important, because the ages of these clusters are well determined and the fact that they lie in the midst of the lithium vs. age trend of the field solar twins suggests that the ages we derived for individual stars are reliable. The Spearman correlation coefficient for the solar twin $\log \epsilon_{\text{Li}}$ -age trend

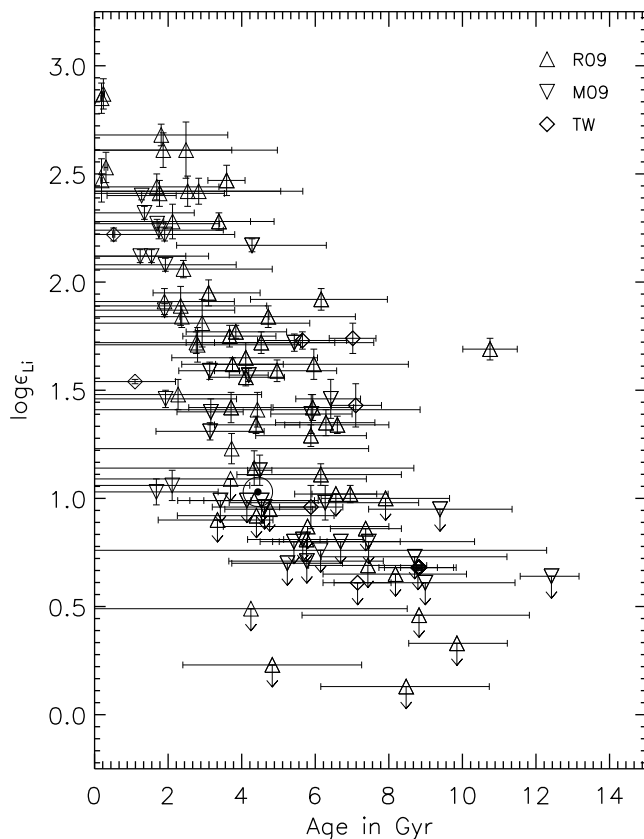


Fig. 2. $\log \epsilon_{\text{Li}}$ vs. age for stars from the three observational sub-samples. Down-arrows denote upper limits. The Sun is marked with \odot .

including the open cluster data is $r_{\text{twin}} = -0.75$. Another interesting thing to point out here is the fact that the Sun (marked with \odot in the figures) fits the trend very well. This leads to the conclusion that the Sun does not have a particularly low lithium abundance compared to stars of similar age, mass, and metallicity.

Figure 3 also compares our observational data with model predictions from Charbonnel & Talon (2005) for different initial rotational velocities of the stars. These hydrodynamical models give predictions for the evolution of surface Li abundance in solar-type stars, accounting self-consistently for element segregation and transport of angular momentum and chemicals by meridional circulation, shear turbulence and internal gravity waves. They agree not only with the general lithium depletion trend observed by us, but it could also explain the relatively large scatter as a result of differences in initial stellar rotational velocities.

3.2. Lithium and planets

In Fig. 4 we plot lithium abundance against age, this time for a sample of metal-rich solar analogs. As metal-rich solar analogs we define stars with $[\text{Fe}/\text{H}] = 0.25 \pm 0.15$ and $M = (1.08 \pm 0.08) M_{\odot}$. We use those criteria because our sub-sample of planet-hosts is biased towards those higher metallicities and masses. In this case we make a distinction between stars that are known to host planets (filled symbols) and those for which planets have not yet been detected (open symbols).

We used a two-dimensional Kolmogorov-Smirnov (KS) test to measure the probability that the samples of metal-rich solar analogs with and without planets in Fig. 4 belong to the same

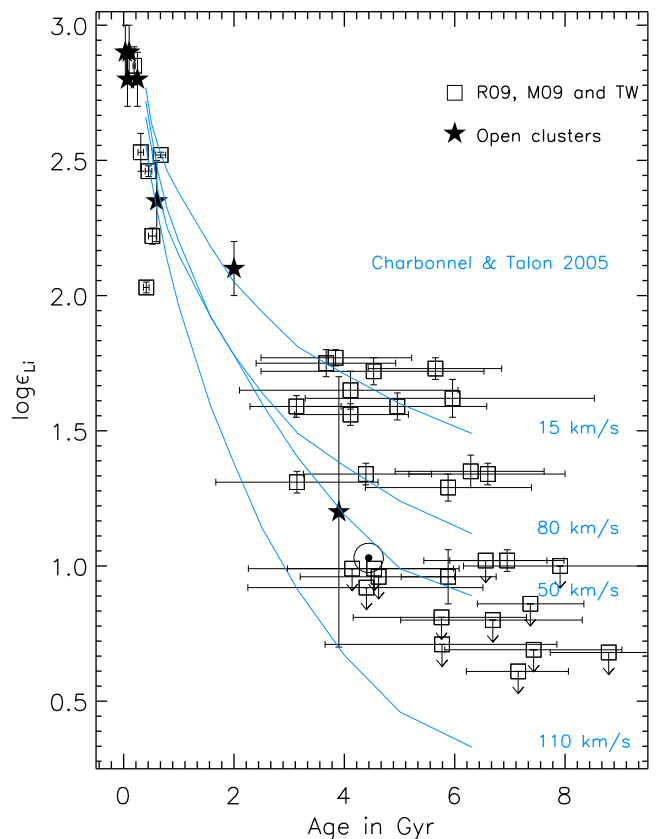


Fig. 3. $\log \epsilon_{\text{Li}}$ vs. age for solar twins from R09, M09, TW and from the solar twins in solar metallicity open clusters. Note the different scale compared to Fig. 2. The solid lines are the predicted values from the models by Charbonnel & Talon (2005) for different initial rotational velocities.

parent population. Using a Monte Carlo simulation, we took into account the errors in lithium abundance and age by choosing random, normally distributed values within each variable's $1\text{-}\sigma$ environment on the linear scale, which means that instead of $\log \epsilon_{\text{Li}}$, we used $10^{\log \epsilon_{\text{Li}} - 12}$, that is $\frac{Z_{\text{Li}}}{n_{\text{H}}}$. The upper limits were accounted for by distributing the values uniformly between 0 and the upper limit.

We averaged the outcome of 1000 KS tests. This gave a probability for our metal-rich solar analogs with planets and those without planets to be part of the same parent sample of $64 \pm 15\%$; if we ignore the error bars and upper limits, this probability goes up to 80%. This is very important for the further analysis of the data, because it tells us that there is no *intrinsic* difference between the two sub-samples. It is highly unlikely that the planet-hosts and comparison stars are different regarding their surface lithium abundance.

The age-lithium correlation coefficient for the solar twins is similar to that corresponding to the metal-rich solar analogs ($r_{\text{twin}} = -0.75$, $r_{\text{analog}} = -0.71$). However, the shapes of those trends are not identical. In the range from 3 to 6 Gyr, in particular, it is clear that for a given age, metal-rich solar analogs have on average lower lithium abundances than solar twins (see also Fig. 5c). This is independent of whether the star has a planet or not. The age-lithium trend in Sun-like stars is thus metallicity dependent. This metallicity effect is predicted by stellar models due to the deeper convection zone in more metal-rich stars (Castro et al. 2009) and has lately been confirmed (see, e.g. do Nascimento et al. 2010, Fig. 5). Note, however, that the mass

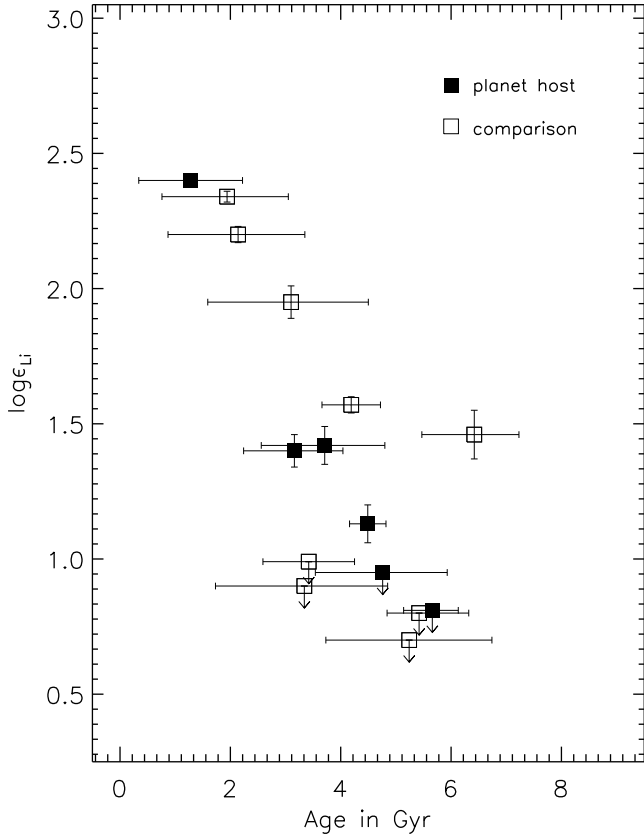


Fig. 4. Same as Fig. 3 but for metal-rich solar analogs ($[\text{Fe}/\text{H}] = 0.25 \pm 0.15$, $M = 1.08 \pm 0.08 M_{\odot}$).

ranges being compared are somewhat different, and that this will have an impact on the lithium evolution of those two samples.

4. Discussion

Recently, it was claimed that planet-harboring solar-type stars show an enhanced lithium depletion and that lithium surface abundances in Sun-like stars do not correlate with stellar ages (Israelian et al. 2009; Sousa et al. 2010, hereafter I09 and S10, respectively).

In Fig. 5, we plot age versus lithium abundance for all 82 stars used in I09 along with the objects from this work (hereafter B10³). With the stellar parameters adopted by I09 we derived the ages for that sample using the same techniques as for our sample; the ages we derive for the I09 sample are given in Table 5. Figure 5 shows the results for all stars panel (a), the solar twins (panel (b)), and the metal-rich solar analogs (panel (c)). We are using the same selection criteria for solar twins and metal-rich solar analogs as in Sect. 3. The agreement between the age-lithium relation found with our sample and that by I09 is excellent, in particular when looking at the solar twin plot. This shows that the stellar parameters used by I09 (which were derived by Sousa et al. 2008) are essentially on the same scale as ours and therefore the combination of both samples for this analysis does not introduce systematic errors. In fact, for the 10 stars in common between our sample and I09 we find differences of 3 ± 20 K in T_{eff} , 0.02 ± 0.04 in $\log g$, 0.003 ± 0.023 in $[\text{Fe}/\text{H}]$,

³ For consistency, we used our LTE lithium abundance in this discussion because the I09 work does not take into account non-LTE corrections.

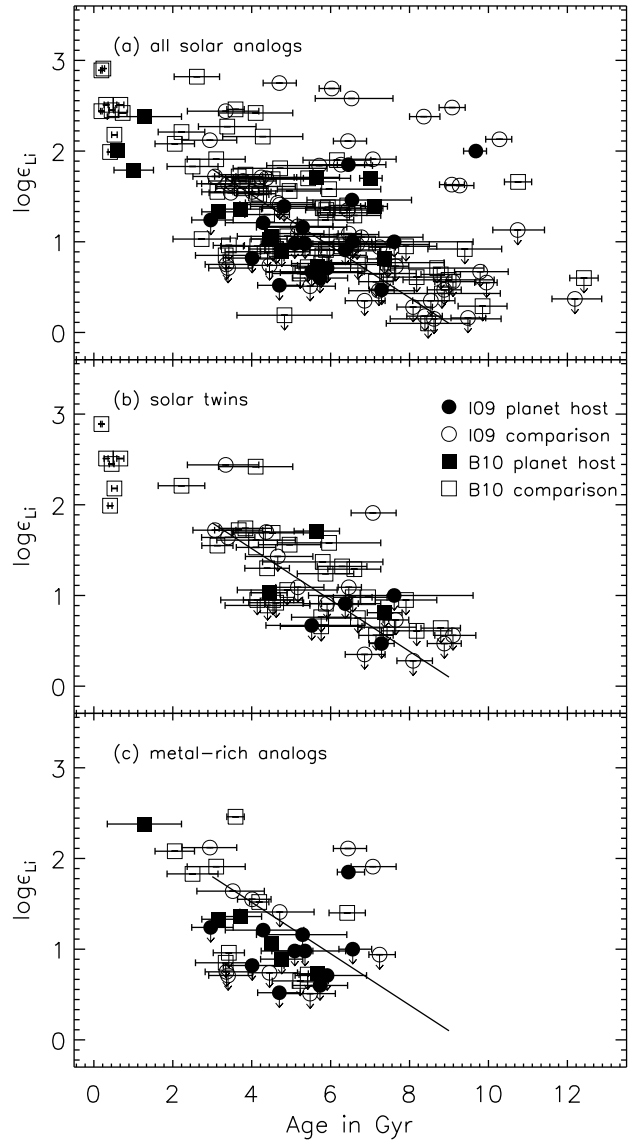


Fig. 5. Comparison between the sample from Israelian et al. (2009, I09) and our sample (B10). The solid line, identically drawn in each panel, is an arbitrary reference line to guide the eye to the different $\log \epsilon_{\text{Li}}$ levels in solar twins and metal-rich solar analogs. Note that for consistency we use the LTE $\log \epsilon_{\text{Li}}$ values here.

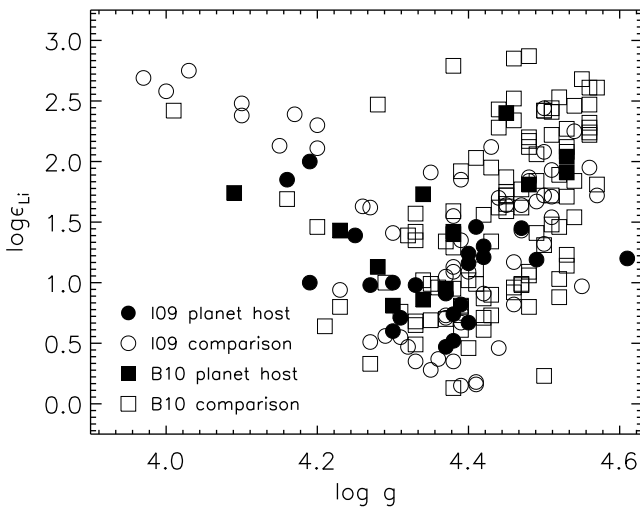
and 0.06 ± 0.11 in $\log \epsilon_{\text{Li}}$ (the latter for the only 3 stars with lithium doublet detection).

In Fig. 5a, ten stars with ages greater than 4 Gyr and higher than average $\log \epsilon_{\text{Li}}$ can be seen above the main locus. Taking a closer look at those “outliers”, the most interesting fact is that they have a particularly low surface gravity ($\log g \simeq 4.1$) compared to the rest of stars. In Fig. 6, we show $\log \epsilon_{\text{Li}}$ vs. $\log g$. The surface lithium abundance on the low- $\log g$ side does not follow the main track, for which $\log \epsilon_{\text{Li}}$ decreases with lower surface gravity, which is essentially the age effect, given that all these stars have similar masses. To exclude the possibility of systematic errors in the analysis of the low $\log g$ outliers, we compared the parameters and in particular their ages with various sources (see Table 3). Our derived ages for these outliers are in reasonably good agreement with respect to the values given in the literature. Only two stars appear to be older than the ages given in the consulted references, but even that difference is only around 2 Gyr and therefore not big enough for these stars to

Table 3. Ages, masses, and lithium abundances for the outliers in Fig. 5a.

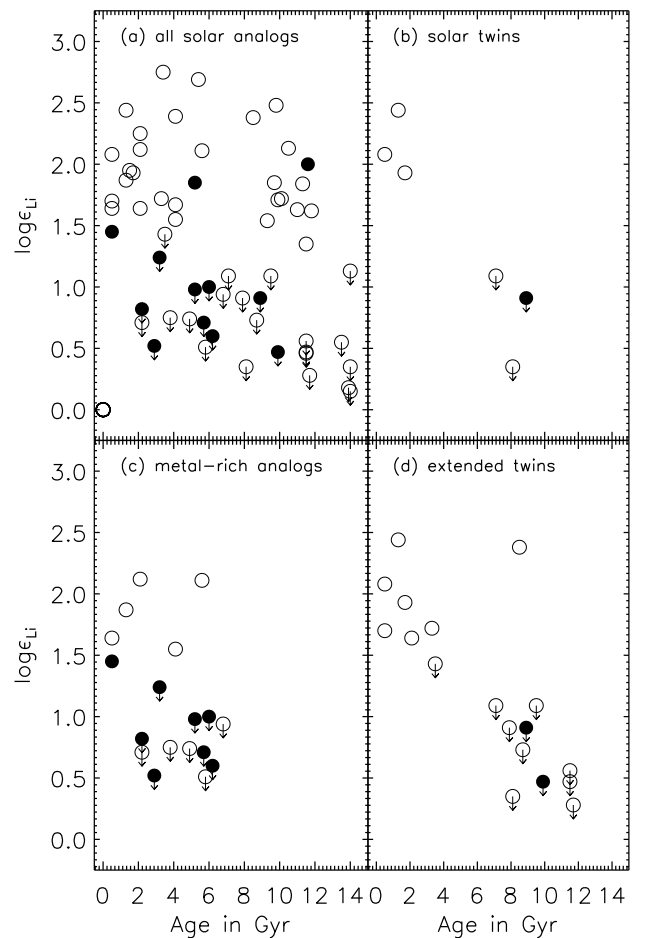
Object	Age in Gyr	mass in M_{\odot}	$\log \epsilon_{\text{Li}}$ in dex	Ages from other sources in Gyr ^a
HD 221420	4.70	1.30	2.75	4.5 (GCS), 4.1 (VF05), 5.1 (RP98)
HD 114613	6.03	1.19	2.69	5.1 (RP98), 5.6 (B07, rot), 4.9 (VF05), 4.9 (RP98)
HD 2151	6.53	1.12	2.58	5.2 (GCS), 5.8 (VF05), 6.7 (V05)
HD 215456	8.36	1.04	2.38	7.3 (GCS), 7.0 (I02)
HD 32724	9.07	0.97	1.63	9.9 (GCS)
HD 4307	9.08	1.01	2.48	7.8 (W04, R'_{HK} , rot), 7.4 (GCS), 6.4 (VF05)
HD 78612	9.27	0.96	1.62	8.8 (GCS)
HD 114729	9.68	0.97	2.00	10.9 (GCS), 6.45 (RP98) [planet-host]
HD 145809	10.28	0.96	2.13	6.9 (W04, R'_{HK} , rot), 7.9 (GCS), 7.4 (VF05)
HD 32923	10.75	0.96	1.66	9.0 (VF05), 6.2 (W04), 9.9 (GCS), >9.5 (S83)

Notes. R'_{HK} denotes ages derived from chromospheric activity, rot denotes ages derived from rotation periods. ^(a) The abbreviations used here are the following: GCS: The Geneva-Copenhagen survey, Nordström et al. (2004), VF05: Valenti & Fischer (2005), RP98: Rocha-Pinto & Maciel (1998), V05: Vardavas (2005), I02: Ibukiyama & Arimoto (2002), W04: Wright et al. (2004) and S83: Soderblom (1983).


Fig. 6. $\log \epsilon_{\text{Li}}$ vs. $\log g$ for the stars from our sample (B10) and I09.

cease being outliers. This leads us to the conclusion that the ages we derived for the I09 sample and the stellar parameters adopted by I09 (mostly derived by Sousa et al. 2008) are correct and the high-lithium envelope in the lithium-age plane is most likely real. Thus, when restricted to a narrow range of T_{eff} around the solar value, $\log g \approx 4.1$ stars have higher lithium abundances than less evolved stars of similar age.

We have examined the results by S10, who claim that there is no correlation between lithium and age in the I09 sample. The S10 sample is basically the same as in I09, but reduced to the 60 stars studied in Sousa et al. (2008) because of the high homogeneity of the stellar parameters. We show their lithium-age trends in Fig. 7. The selection criteria we used for the solar twins and the metal-rich solar analogs are the same as in Fig. 5. However, this time we are using the masses and ages determined by S10. Although their full sample appears to show no correlation (Fig. 7a), the solar twin sample shows a clear trend between lithium and age. Note that the one planet-host in this sample has a low lithium abundance because of its old


Fig. 7. $\log \epsilon_{\text{Li}}$ vs. age for the S10 sample. The selection criteria for the four panels are given in the text. Masses and ages adopted to make this figure are from S10.

age and not the fact that it hosts a planet. There is no clear correlation between lithium and age for the metal-rich solar analog

Table 4. Specifications for the different samples^b.

HIP	HD	T_{eff}	$\sigma(T_{\text{eff}})$	$\log g$	$\sigma(\log g)$	[Fe/H]	$\sigma(\text{Fe}/\text{H})$	$\log \epsilon_{\text{Li}}$ (LTE)	$\log \epsilon_{\text{Li}}$ (NLTE)	$\sigma(\log \epsilon_{\text{Li}})$	Mass	$\sigma(m)$	Age	$\sigma(\tau)$	Source(τ)	Parameters	Planets
Sun	Sun	5777	–	4.44	–	0.000	–	1.03	1.07	0.04	1.00	0.01	4.5	0.5	iso	–	yes
348	225194	5777	40	4.41	0.07	-0.130	0.024	1.08	1.11	0.05	0.97	0.01	6.2	1.5	iso	R09	no
996	804	5860	41	4.38	0.07	0.000	0.022	1.56	0.95	0.05	1.03	0.01	5.1	1.1	iso	R09	no
1499	1461	5756	44	4.37	0.05	0.189	0.015	0.89	1.00	-1.00	1.06	0.01	4.8	0.6	iso	R09+V05+LH06+T07+S08	yes
2131	236416	5720	41	4.38	0.07	-0.210	0.026	0.10	0.13	-1.00	0.92	0.01	8.9	1.3	iso	R09	no
2894	–	5820	44	4.54	0.07	-0.030	0.025	1.81	1.84	0.05	1.02	0.01	1.6	0.8	iso	R09	no
4909	6204	5836	54	4.44	0.07	0.020	0.024	2.42	2.43	0.06	1.03	0.01	0.7	0.2	x-ray	R09+G09	no
5134	6470	5779	38	4.49	0.07	-0.190	0.023	1.81	1.84	0.05	0.97	0.01	4.1	1.9	iso	R09	no
6407	8291	5787	25	4.47	0.03	-0.090	0.011	1.74	1.77	0.03	0.99	0.01	3.8	0.8	iso	R09	no
7245	9446	5843	47	4.53	0.07	0.100	0.023	1.87	1.91	0.06	1.07	0.01	1.3	0.7	iso	R09	yes
8507	11195	5720	55	4.44	0.08	-0.080	0.026	1.58	1.62	0.07	0.96	0.01	5.6	2.0	iso	R09	no
8841	–	5676	45	4.50	0.06	-0.120	0.021	0.19	0.23	-1.00	0.95	0.01	4.3	1.8	iso	R09	no
9349	12264	5825	28	4.49	0.06	0.010	0.017	2.03	2.06	0.04	1.03	0.01	2.5	1.2	iso	R09+T07	no
10710	–	5817	43	4.39	0.06	-0.130	0.022	1.90	1.92	0.05	0.98	0.01	6.5	1.1	iso	R09	no
11072	14802	5897	84	4.01	0.058	-0.037	0.057	2.42	2.42	0.02	1.15	0.02	0.7	0.1	rot	TW+B07	no
11728	15632	5738	30	4.37	0.05	0.045	0.019	1.29	1.34	0.04	0.99	0.01	6.9	0.8	iso	R09+T07	no
11915	16008	5793	43	4.45	0.06	-0.050	0.021	1.69	1.72	0.05	1.00	0.01	4.3	1.6	iso	R09	no
12186	16417	5812	34	4.09	0.05	0.094	0.04	1.70	1.74	0.07	1.11	0.01	7.0	0.4	iso	TW+V05+S08	yes
14614	19518	5803	28	4.47	0.03	-0.104	0.016	1.59	1.62	0.03	0.99	0.01	3.6	0.9	iso	R09+T07+TW	no
14632	19373	6026	42	4.28	0.05	0.136	0.019	2.46	2.47	0.07	1.17	0.01	3.7	0.3	iso	R09+V05	unknown
15457	20630	5771	65	4.56	0.016	0.078	0.041	2.18	2.22	0.03	1.02	0.01	0.5	0.0	rot	TW+V05	unknown
18261	24552	5891	34	4.44	0.05	0.002	0.016	2.27	2.28	0.04	1.05	0.01	3.1	1.1	iso	R09+T07	no
22263	30495	5826	48	4.54	0.012	0.005	0.029	2.45	2.46	0.02	1.02	0.01	0.5	0.1	rot	TW+V05	unknown
22528	–	5683	52	4.33	0.10	-0.350	0.035	0.46	0.49	-1.00	0.87	0.01	12.2	1.5	iso	R09	no
23835	32923	5723	33	4.16	0.05	-0.184	0.017	1.66	1.69	0.05	0.96	0.01	10.7	0.4	iso	R09+V05	unknown
25670	36152	5755	37	4.38	0.05	0.071	0.017	1.24	1.29	0.05	1.01	0.01	6.0	0.9	iso	R09+T07	unknown
28336	40620	5713	61	4.53	0.08	-0.170	0.027	1.19	1.23	0.07	0.95	0.01	4.0	1.8	iso	R09	no
29255	42807	5715	61	4.41	0.037	-0.005	0.036	1.99	2.03	0.02	0.97	0.01	0.4	0.0	rot	TW+B07	no
30037	45021	5690	30	4.42	0.06	0.05	0.03	0.66	0.71	-1.00	0.98	0.01	5.9	1.4	iso	M09	no
30502	45346	5745	25	4.47	0.05	-0.01	0.02	0.95	0.99	-1.00	1.00	0.01	3.8	1.4	iso	M09	no
36512	59711	5740	15	4.50	0.03	-0.092	0.02	1.27	1.31	0.04	0.99	0.01	2.7	1.0	iso	M09+V07+S08	unknown
38072	63487	5839	68	4.53	0.11	0.060	0.037	1.67	1.71	0.08	1.05	0.01	2.4	1.2	iso	R09	no
38228	63433	5693	58	4.52	0.07	0.007	0.025	2.51	2.53	0.07	0.99	0.01	0.3	0.0	rot	R09+V05, τ from G00	unknown
39748	67578	5835	30	4.48	0.06	-0.20	0.03	2.16	2.17	0.03	0.98	0.01	3.8	1.6	iso	M09	no
41317	71334	5724	15	4.46	0.03	-0.044	0.02	0.92	0.96	-1.00	0.98	0.01	4.7	0.8	iso	M09+V05+S08	unknown
42438	72905	5864	47	4.46	0.09	-0.052	0.026	2.89	2.85	0.07	1.02	0.01	0.2	0.0	rot	R09+TW	no
43190	75288	5775	30	4.37	0.06	0.12	0.03	0.65	0.70	-1.00	1.04	0.01	5.3	0.9	iso	M09	no
44324	77006	5934	49	4.51	0.06	-0.020	0.019	2.41	2.41	0.06	1.07	0.01	1.5	0.6	iso	R09+T07	no
44713	78429	5784	35	4.36	0.027	0.096	0.024	0.91	0.96	0.10	1.03	0.01	5.8	0.6	iso	TW + VF05 + S08	unknown
44935	78534	5800	25	4.41	0.05	0.07	0.02	0.95	0.99	-1.00	1.03	0.01	4.6	1.0	iso	M09	no
44997	78660	5782	29	4.52	0.04	0.033	0.02	0.99	1.03	0.06	1.03	0.01	1.5	0.5	iso	M09 + T07	no
46066	80533	5709	65	4.49	0.12	-0.070	0.039	1.37	1.41	0.08	0.96	0.01	5.2	2.3	iso	R09	no
46126	81700	5890	30	4.48	0.06	0.14	0.03	2.17	2.20	0.03	1.09	0.01	1.7	0.8	iso	M09	no
47990	84705	5910	40	4.53	0.08	0.12	0.03	2.24	2.27	0.02	1.10	0.01	0.8	0.4	iso	M09	no
49572	–	5831	52	4.33	0.06	0.010	0.021	1.32	1.35	0.06	1.02	0.01	6.6	0.8	iso	R09	no
49756	88072	5804	52	4.45	0.07	0.041	0.023	1.61	1.65	0.07	1.03	0.01	3.6	1.6	iso	R09+V05+T07	unknown
50826	–	5725	30	4.47	0.06	-0.28	0.03	0.95	0.98	0.08	0.92	0.01	6.1	1.8	iso	M09	no
51258	90722	5720	25	4.23	0.05	0.360	0.03	0.72	0.80	-1.00	1.17	0.02	5.1	0.2	iso	M09+V05	unknown
52040	91909	5785	44	4.51	0.06	-0.090	0.021	1.69	1.72	0.05	0.99	0.01	3.0	1.2	iso	R09	no

Table 4. continued.

HIP	HD	T_{eff}	$\sigma(T_{\text{eff}})$	$\log g$	$\sigma(\log g)$	[Fe/H]	$\sigma(\text{[Fe/H]})$	$\log \epsilon_{\text{Li}}$ (LTE)	$\log \epsilon_{\text{Li}}$ (NLTE)	$\sigma(\log \epsilon_{\text{Li}})$	Mass	$\sigma(m)$	Age	$\sigma(\tau)$	Source(τ)	Parameters	Planets
52137	92074	5842	69	4.56	0.08	0.070	0.026	2.25	2.28	0.08	1.06	0.01	0.9	0.5	iso	R09	no
53721	95128	5916	53	4.48	0.015	0.027	0.038	1.79	1.81	0.02	1.07	0.01	1.0	0.5	iso + rot	TW+V05+S05+M08	yes
54102	96116	5870	30	4.51	0.06	0.04	0.03	2.20	2.22	0.03	1.06	0.01	1.6	0.7	iso	M09	no
55409	98649	5760	25	4.52	0.05	-0.01	0.02	0.84	0.88	0.07	1.01	0.01	2.1	0.8	iso	M09	no
55459	98618	5838	21	4.42	0.03	0.038	0.012	1.53	1.56	0.04	1.03	0.01	4.1	0.7	iso	R09+V05+M06+T07	unknown
56948	101364	5795	23	4.43	0.03	0.023	0.014	1.30	1.34	0.04	1.01	0.01	4.4	0.7	iso	R09+MR07+T09	unknown
56997	101501	5559	65	4.53	0.08	-0.030	0.027	1.08	1.14	0.08	0.94	0.01	4.6	2.1	iso	R09+V05	unknown
57291	102117	5690	22	4.30	0.04	0.304	0.03	0.73	0.81	-1.00	1.11	0.01	5.6	0.2	iso	M09+V05+S08	yes
59357	105779	5810	30	4.45	0.06	-0.24	0.03	1.70	1.72	0.04	0.95	0.01	5.5	1.5	iso	M09	no
59610	106252	5899	62	4.34	0.041	-0.034	0.041	1.71	1.73	0.04	1.04	0.01	5.7	0.7	iso	TW+V05	yes
60081	107148	5811	21	4.38	0.04	0.315	0.03	1.33	1.40	0.06	1.12	0.01	3.4	0.5	iso	M09+V05+S08	yes
60314	107633	5874	72	4.52	0.10	0.110	0.033	1.85	1.89	0.09	1.07	0.01	1.9	0.9	iso	R09	no
60370	107692	5897	25	4.46	0.05	0.171	0.03	2.31	2.34	0.02	1.11	0.01	1.6	0.8	iso	M09+V05	unknown
60653	108204	5725	30	4.38	0.06	-0.29	0.03	0.92	0.95	-1.00	0.90	0.01	9.6	1.2	iso	M09	no
62175	110869	5849	51	4.43	0.06	0.140	0.021	1.91	1.95	0.06	1.08	0.01	2.9	1.2	iso	R09+T07	no
64150	114174	5755	41	4.39	0.05	0.056	0.016	0.76	0.81	-1.00	1.00	0.01	5.9	1.0	iso	R09+V05+T07	unknown
64497	114826	5860	110	4.56	0.11	0.120	0.037	2.60	2.61	0.13	1.07	0.02	1.3	0.8	iso	R09	no
64713	115169	5815	25	4.52	0.05	-0.01	0.02	1.43	1.46	0.04	1.03	0.01	1.7	0.8	iso	M09	no
64794	115382	5743	61	4.33	0.08	-0.100	0.027	0.61	0.65	-1.00	0.96	0.01	8.8	1.0	iso	R09	no
64993	115739	5875	30	4.56	0.06	0.09	0.03	2.30	2.32	0.03	1.08	0.01	0.9	0.5	iso	M09	no
66618	118475	5951	25	4.35	0.05	0.135	0.03	0.96	0.99	-1.00	1.12	0.01	3.6	0.5	iso	M09+V05	unknown
66885	119205	5685	30	4.48	0.06	-0.38	0.03	0.77	0.80	-1.00	0.88	0.01	7.4	1.9	iso	M09	no
69063	123152	5670	30	4.31	0.06	-0.45	0.03	0.74	0.76	-1.00	0.83	0.01	14.1	0.7	iso	M09	no
71683	128620	5840	22	4.33	0.04	0.228	0.03	1.52	1.57	0.03	1.11	0.01	4.3	0.3	iso	M09+V05+PM08	unknown
72659	131156	5517	67	4.56	0.09	-0.117	0.033	2.44	2.47	0.10	0.91	0.01	0.2	0.0	rot	R09+V05	unknown
73815	133600	5803	33	4.34	0.05	0.020	0.016	0.98	1.02	-1.00	1.01	0.01	6.8	0.6	iso	R09+MR07	no
74341	134902	5853	57	4.51	0.08	0.090	0.026	1.44	1.48	0.07	1.07	0.01	1.9	0.9	iso	R09	no
74389	134664	5859	24	4.48	0.04	0.105	0.03	2.08	2.12	0.03	1.07	0.01	1.6	0.7	iso	M09+S08	unknown
75923	138159	5775	25	4.56	0.05	-0.02	0.02	2.21	2.24	0.04	1.02	0.01	0.9	0.2	iso	M09	no
77052	140538	5697	33	4.54	0.023	0.035	0.023	1.49	1.54	0.01	1.01	0.01	0.6	0.4	iso	TW+V05	unknown
77466	-	5700	56	4.40	0.09	-0.280	0.028	0.43	0.46	-1.00	0.90	0.01	9.3	1.9	iso	R09	no
77740	141937	5900	19	4.45	0.04	0.125	0.03	2.38	2.40	0.02	1.09	0.01	1.3	0.9	iso + rot	M09+M05+S05+V05+LH06+S08	yes
77883	142331	5695	25	4.39	0.05	0.04	0.02	0.75	0.80	-1.00	0.98	0.01	7.0	0.9	iso	M09	no
78028	-	5879	98	4.57	0.12	-0.030	0.041	1.79	1.81	0.11	1.04	0.02	1.8	1.0	iso	R09	no
78680	144270	5923	67	4.57	0.08	-0.000	0.027	2.61	2.61	0.08	1.06	0.01	0.6	0.4	iso	R09	no
79186	145514	5709	48	4.27	0.08	-0.120	0.024	2.09	0.33	-1.00	0.95	0.01	10.3	0.7	iso	R09	no
79304	145478	5945	30	4.53	0.06	0.11	0.03	2.09	2.12	0.03	1.11	0.01	0.4	0.2	iso	M09	no
79578	145825	5860	33	4.53	0.07	0.072	0.03	2.05	2.08	0.03	1.07	0.01	1.3	0.6	iso	M09+V05	unknown
79672	146233	5822	9	4.45	0.02	0.051	0.02	1.55	1.59	0.04	1.04	0.01	3.1	0.5	iso	M09+TW+S08	unknown
80337	147513	5881	33	4.53	0.024	0.033	0.022	2.01	2.04	0.02	1.06	0.03	0.6	0.1	rot	TW (S+N+HARPS)+V05+S08+B07	yes
81512	-	5790	58	4.46	0.07	-0.020	0.025	0.89	0.92	-1.00	1.01	0.01	4.0	1.7	iso	R09	no
82853	150027	5640	30	4.21	0.06	-0.18	0.03	0.60	0.64	-1.00	0.92	0.01	12.5	0.5	iso	M09	no
83601	154417	6071	43	4.38	0.08	0.048	0.028	2.82	2.79	0.06	1.13	0.01	2.4	1.1	iso	R09+V05	unknown
83707	152441	5880	30	4.45	0.06	0.15	0.03	1.83	1.87	0.03	1.10	0.01	2.3	1.0	iso	M09	no
85042	157347	5692	37	4.39	0.022	0.037	0.026	0.56	0.61	-1.00	0.98	0.01	7.2	0.5	iso	TW+V05+S08	unknown
85272	156922	5700	30	4.42	0.06	-0.34	0.03	0.58	0.61	-1.00	0.88	0.01	9.4	1.4	iso	M09	no
85285	157691	5730	30	4.43	0.06	-0.39	0.03	0.71	0.73	-1.00	0.88	0.01	8.8	1.5	iso	M09	no

Table 4. continued.

HIP	HD	T_{eff}	$\sigma(T_{\text{eff}})$	$\log g$	$\sigma(\log g)$	[Fe/H]	$\sigma(\text{[Fe/H]})$	$\log \epsilon_{\text{Li}}(\text{L.TE})$	$\log \epsilon_{\text{Li}}(\text{NLTE})$	$\sigma(\log \epsilon_{\text{Li}})$	Mass	$\sigma(m)$	Age	$\sigma(\tau)$	Source(τ)	Parameters	Planets
86796	160691	5809	22	4.28	0.04	0.298	0.03	1.06	1.13	0.07	1.15	0.01	4.6	0.2	iso	M09+V05+S08	yes
88194	164595	5735	21	4.40	0.03	-0.071	0.010	0.98	1.02	0.04	0.96	0.01	7.3	0.6	iso	R09+V05+T07	unknown
88427	–	5810	57	4.42	0.07	-0.160	0.025	0.85	0.87	-1.00	0.97	0.01	5.7	1.5	iso	R09	no
89162	165357	5835	30	4.32	0.06	0.07	0.03	1.35	1.39	0.09	1.05	0.01	6.0	0.6	iso	M09	no
89443	238838	5796	73	4.48	0.12	-0.020	0.038	1.06	1.09	-1.00	1.01	0.01	4.4	1.9	iso	R09	no
89650	167060	5855	25	4.48	0.05	0.02	0.02	1.03	1.06	0.07	1.05	0.01	2.2	1.0	iso	M09	no
91332	171918	5775	25	4.20	0.05	0.206	0.03	1.40	1.46	0.09	1.12	0.02	6.4	0.7	iso	M09+V05	unknown
96402	184768	5713	49	4.33	0.032	-0.029	0.030	0.64	0.68	-1.00	0.97	0.01	8.7	0.7	iso	TW+T07	no
96901	186427	5737	28	4.34	0.04	0.055	0.016	1.38	1.42	-1.00	1.00	0.01	7.5	0.5	iso	R09+V05+LH06+T07	yes
96895	186408	5808	39	4.33	0.05	0.097	0.020	0.81	0.86	0.06	1.05	0.01	6.0	0.6	iso	R09+V05+LH06	unknown
100963	195034	5802	17	4.45	0.03	0.008	0.013	1.72	1.75	0.05	1.02	0.01	3.6	0.8	iso	R09+T07+T09	no
100970	195019	5823	40	4.23	0.026	0.083	0.025	1.39	1.43	0.10	1.06	0.01	7.2	0.4	iso	TW+V05	yes
102152	197027	5737	47	4.35	0.06	-0.010	0.022	0.65	0.69	-1.00	0.98	0.01	7.7	0.9	iso	R09+M09	no
104504	201422	5836	48	4.50	0.06	-0.160	0.022	2.42	2.42	0.06	1.00	0.02	3.0	1.4	iso	R09	no
107350	206860	6015	50	4.48	0.07	-0.020	0.019	2.91	2.87	0.07	1.09	0.01	0.2	0.0	rot	R09+V05	unknown
108708	209096	5875	51	4.51	0.07	0.150	0.024	2.42	2.44	0.06	1.10	0.01	1.3	0.6	iso	R09	no
108996	209562	5838	56	4.50	0.08	0.060	0.027	2.40	2.42	0.07	1.05	0.01	2.3	1.1	iso	R09	no
109110	209779	5817	60	4.46	0.033	0.062	0.030	2.51	2.52	0.01	1.04	0.01	0.7	0.1	rot	TW+V05+T07+B07	unknown
109931	–	5739	74	4.29	0.08	0.040	0.026	0.95	1.00	-1.00	1.00	0.01	8.2	0.9	iso	R09	no
113357	217014	5803	47	4.38	0.05	0.221	0.017	1.36	1.42	0.07	1.09	0.01	3.9	0.7	iso	R09+V05+LH06	yes
115604	–	5821	51	4.43	0.06	0.140	0.019	0.85	0.90	-1.00	1.07	0.01	3.1	1.2	iso	R09	no
118159	224448	5905	44	4.55	0.07	-0.010	0.022	2.69	2.68	0.05	1.06	0.01	0.8	0.4	iso	R09	no

Notes. ^(b) The abbreviations of the sources in Table 4 are the following: R09, M09 and TW are from Ramírez et al. (2009), Meléndez et al. (2009), Meléndez et al. (2010) and this work, as before. M06 is Meléndez et al. (2006), V05 is Valenti & Fischer (2005), S08 is Sousa et al. (2008), B07 Barnes (2007), LH06 Luck & Heiter (2006), PM08 Porto de Mello et al. (2008), T07 and T09 are Takeda et al. (2007) and Takeda & Tajitsu (2009), respectively, G00 is Gaidos et al. (2000) and MR07 is Meléndez & Ramírez (2007). S05 is Saffe et al. (2005), G09 is Guinan & Engle (2009), and M08 Mamajek & Hillenbrand (2008). The -1 in $\sigma(\log \epsilon_{\text{Li}})$ denotes upper limits.

Table 5. Sample used in I09. Masses and ages are from this work.

Star name or HIP	HD	Mass	$\sigma(m)$	Age	$\sigma(\tau)$	Star name or HIP	HD	Mass	$\sigma(m)$	Age	$\sigma(\tau)$
WASP 5	–	0.99	0.06	7.9	3.3	52409	92788	1.08	0.01	3.8	1.0
XO-1	–	1.01	0.01	2.3	1.2	53837	95521	0.98	0.01	3.4	1.1
1499	1461	1.07	0.01	4.5	0.6	54287	96423	1.01	0.01	7.2	0.6
1954	2071	0.97	0.01	4.6	1.1	54400	96700	0.97	0.01	6.6	0.6
2021	2151	1.12	0.08	6.7	1.4	97998	97998	0.90	0.01	1.9	0.6
5339	4307	1.01	0.01	9.0	0.4	60081	107148	1.12	0.01	3.0	0.6
6455	8406	0.98	0.01	3.0	0.6	60729	108309	1.05	0.01	7.5	0.3
8798	11505	0.93	0.01	8.6	0.6	62345	111031	1.10	0.01	3.4	0.8
9381	12387	0.91	0.01	9.1	1.7	64408	114613	1.20	0.02	5.9	0.3
9683	12661	1.10	0.03	4.5	1.3	64459	114729	0.97	0.01	9.7	0.2
12048	16141	1.09	0.01	6.9	0.3	64550	114853	0.92	0.01	7.4	0.9
12186	16417	1.12	0.01	6.7	0.2	65036	115585	1.13	0.03	5.3	0.5
14501	19467	0.94	0.01	10.0	0.3	71683	128620	1.17	0.07	4.1	1.5
15442	20619	0.94	0.01	3.9	1.2	74500	134987	1.10	0.02	5.4	0.5
15330	20766	0.94	0.02	3.4	1.7	78330	143114	0.88	0.01	9.9	0.8
15527	20782	0.98	0.01	7.3	0.3	78459	143761	0.98	0.02	6.1	2.6
16365	21938	0.86	0.01	10.8	0.7	79524	145809	0.96	0.01	10.3	0.3
19925	27063	1.01	0.01	4.2	1.2	79672	146233	1.03	0.01	3.3	0.8
20625	28471	0.97	0.01	7.7	0.3	83906	154962	1.22	0.03	4.7	0.8
20677	28701	0.89	0.01	9.5	0.5	160691	160691	1.14	0.02	4.8	0.3
23627	32724	0.97	0.01	9.2	0.3	95962	183658	1.01	0.01	5.3	0.7
22504	34449	1.02	0.01	1.5	0.8	96901	186427	1.02	0.02	5.0	1.9
25670	36152	1.05	0.01	2.6	0.9	97336	187123	1.07	0.01	3.5	1.5
26737	37962	0.94	0.01	5.2	1.8	97769	188015	1.10	0.02	1.8	0.9
27435	38858	0.95	0.01	3.3	0.7	98959	189567	0.92	0.01	8.4	0.4
30243	44420	1.11	0.01	3.5	0.6	98589	189625	1.09	0.01	2.5	1.0
30104	44594	1.08	0.00	4.1	0.5	102664	198075	0.99	0.01	2.3	1.0
30476	45289	0.97	0.00	8.8	0.3	104903	202206	1.09	0.01	1.4	0.6
34065	53705	0.97	0.01	6.8	2.3	106006	204313	1.06	0.01	4.6	0.5
36512	59711A	0.96	0.01	5.3	1.0	108468	208704	0.99	0.01	6.6	0.3
39417	66428	1.09	0.02	5.8	1.0	109821	210918	0.96	0.01	8.2	0.4
43726	76151	1.05	0.01	1.5	0.5	110109	211415	0.96	0.01	6.5	1.2
43686	76700	1.17	0.07	4.5	1.2	112414	215456	1.04	0.01	8.4	0.4
44713	78429	1.02	0.01	7.0	0.5	113357	217014	1.08	0.02	3.4	1.6
44890	78538	1.01	0.01	2.5	1.1	–	219542	1.04	0.02	4.6	1.5
44860	78558	0.85	0.01	12.5	0.7	115577	220507	0.98	0.01	9.3	0.5
44896	78612	0.96	0.01	9.4	0.3	116250	221420	1.29	0.06	4.7	0.7
46007	81110	1.11	0.01	0.4	0.1	116852	222480	1.15	0.03	5.6	0.8
49728	88084	0.97	0.01	6.2	0.8	116906	222582	0.99	0.01	6.7	0.8
50534	89454	1.03	0.01	3.0	1.1	117320	223171	1.09	0.01	6.7	0.3
52369	92719	1.01	0.01	1.6	0.9	118123	224393	0.92	0.01	3.6	1.0

sample in this case, but this could be due to uncertain ages. Since the solar twin sample includes only 6 stars, we define another sample of “extended solar twins” with $[\text{Fe}/\text{H}] = 0.0 \pm 0.1$ and $M = 1.00 \pm 0.10 M_{\odot}$. The resulting figure shows a very definite trend of $\log \epsilon_{\text{Li}}$ with age and only a single outlier appears. This outlier (HD 215456), however, shows a relatively low $\log g$ of 4.10 (and an almost solar mass of $1.04 M_{\odot}$).

We have also examined the lithium vs. effective temperature diagram presented by I09. As shown in Fig. 8a, they found that almost all stars with a high lithium abundance ($\log \epsilon_{\text{Li}} \gtrsim 1.5$ dex) have not been shown to be planet hosts yet, whereas planet hosts and objects where no planets have been found are distributed quite equally below that lithium abundance, although the high number of upper limits makes a direct comparison difficult. In order to make a more robust comparison, we have restricted the comparison sample using the following criteria: we only considered comparison objects within a 2σ range in $[\text{Fe}/\text{H}]$, $\log g$, and T_{eff} around planet hosts, where σ are the average values of the uncertainties in the stellar parameters given by Sousa et al. (2008). In this way, we make sure that all stars lie within the same region of parameter space and are not influenced by the age or metallicity effects we find. Note that we do not

restrict the lithium range, only metallicity, surface gravity and effective temperature. Using this selection allows for a homogeneous and unbiased comparison. When we restrict the parameter range covered by the comparison stars as described above, the lithium-planet connection disappears; as seen in Fig. 8b, it is not possible to conclude on stronger lithium depletion in planet hosts compared to other stars. We stress that this figure is plotted directly from the I09 data without further manipulation or use of new parameters.

Three systematic biases have led I09 and S10 to conclude that solar-type planet-hosts feature an enhanced lithium depletion and that there is no age dependence:

1. at $[\text{Fe}/\text{H}] \simeq 0.0$, the existing HARPS sample of solar analogs with planets are on average older and therefore more depleted in lithium than non-planet-hosts, but not because they have planets;
2. at higher $[\text{Fe}/\text{H}]$, where most of the I09 planet-hosts concentrate, there is a slightly different $\log \epsilon_{\text{Li}}$ vs. age trend such that, at a given age in the 3–6 Gyr range, metal-rich solar analogs are more lithium-poor compared to solar metallicity ones. This is true for both planet-hosts as well as single stars;

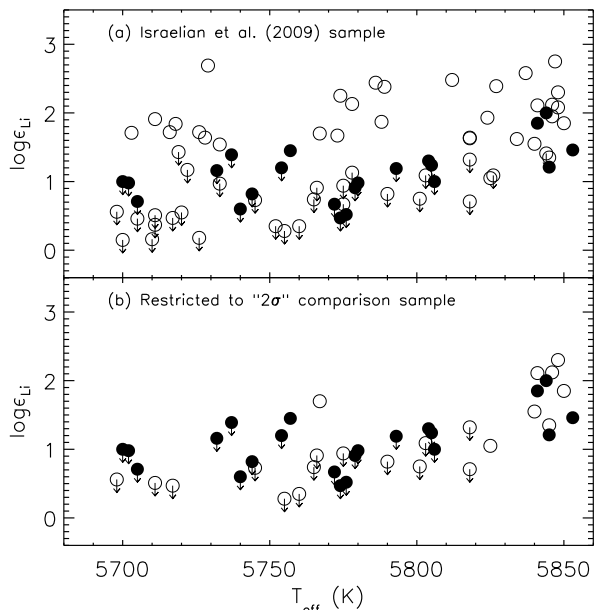


Fig. 8. Lithium abundance as a function of T_{eff} in stars with and without detected planets from the I09 sample. Filled and open circles represent stars with and without detected planets, respectively. In the upper panel the original comparison made is shown, which is not appropriate because the sample being compared span different ranges in evolutionary phases and metallicities. A less biased comparison is shown in the bottom panel, where we only plot stars without detected planets with stellar parameters (T_{eff} , $\log g$, $[\text{Fe}/\text{H}]$) within 2σ of the planet-hosting stars. When a proper comparison is made, i.e., using stars with similar fundamental parameters, lithium is not abnormally low in stars with detected giant planets.

3. I09 and S10 samples include a number of peculiarly high lithium abundance and relatively low $\log g$ (≈ 4.1) stars; only one of them is a planet host.

The apparently lower lithium abundances of planet-hosts found by I09 can thus be fully explained by a combination of age and metallicity effects, not separately but through the age vs. lithium relation.

5. Conclusions

1. In stars of solar mass and solar metallicity, it is clear that older stars have experienced more surface lithium depletion. Both the overall lithium-age trend as well as the scatter that we observe in this sample of stars can be explained by the theoretical models by Charbonnel & Talon (2005).
2. Metal-rich ($[\text{Fe}/\text{H}] \sim 0.25$) solar analogs ($M \sim 1.08 M_{\odot}$) also exhibit a lithium-age trend, which is different from that seen in $1 M_{\odot}$, $[\text{Fe}/\text{H}] = 0.0$ stars. At any given age in the 3 to 6 Gyr range, the metal-rich solar analogs are more lithium-poor. This is true for both planet-hosts and single stars.
3. For solar-like stars, the lithium vs age trends for planet-hosts and stars where no planets have been found are statistically identical. Thus, the presence of a planet does not influence the observed surface lithium abundance.
4. A number of solar-like stars with unusually high lithium abundance for their age are present in the field. We note that all of them have relatively low $\log g \approx 4.1$. We intend to pursue further observational work to better understand this small group of relatively low surface gravity and peculiarly high lithium abundance.

Acknowledgements. We thank G. Israelian for sending us the lithium abundance data from I09.

References

- Agüeros, M. A., Anderson, S. F., Covey, K. R., et al. 2009, *ApJS*, 181, 444
 Allende Prieto, C., Barklem, P. S., Lambert, D. L., & Cunha, K. 2004, *A&A*, 420, 183
 Asplund, M., Grevesse, N., Sauval, A. J., & Scott, P. 2009, *ARA&A*, 47, 481
 Barnes, S. A. 2007, *ApJ*, 669, 1167
 Bouvier, J. 2008, *A&A*, 489, L53
 Castro, M., Vauclair, S., Richard, O., & Santos, N. C. 2008, *Mem. Soc. Astron. Ital.*, 79, 679
 Castro, M., Vauclair, S., Richard, O., & Santos, N. C. 2009, *A&A*, 494, 663
 Castro, M., do Nascimento, J. D., Biazzo, K., Meléndez, J., & de Medeiros, J. R. 2010, *A&A*, submitted
 Charbonnel, C., & Talon, S. 2005, *Science*, 309, 2189
 D’Antona, F., & Mazzitelli, I. 1984, *A&A*, 138, 431
 do Nascimento, Jr., J. D., Castro, M., Meléndez, J., et al. 2009, *A&A*, 501, 687
 do Nascimento, Jr., J. D., da Costa, J. S., & De Medeiros, J. R. 2010 [arXiv:1006.3861]
 Ford, A., Jeffries, R. D., James, D. J., & Barnes, J. R. 2001, *A&A*, 369, 871
 Ford, A., Jeffries, R. D., & Smalley, B. 2005, *MNRAS*, 364, 272
 Gaidos, E. J., Henry, G. W., & Henry, S. M. 2000, *AJ*, 120, 1006
 Gonzalez, G. 2008, *MNRAS*, 386, 928
 Gonzalez, G., Carlson, M. K., & Tobin, R. W. 2010, *MNRAS*, 403, 1368
 Guinan, E. F., & Engle, S. G. 2009, in *IAU Symp.*, 258, 395
 Gustafsson, B., Edvardsson, B., Eriksson, K., et al. 2008, *A&A*, 486, 951
 Ibukiyama, A., & Arimoto, N. 2002, *A&A*, 394, 927
 Israelian, G., Santos, N. C., Mayor, M., & Rebolo, R. 2001, *Nature*, 411, 163
 Israelian, G., Delgado Mena, E., Santos, N. C., et al. 2009, *Nature*, 462, 189
 Jones, B. F., Fischer, D., Shetrone, M., & Soderblom, D. R. 1997, *AJ*, 114, 352
 Kurucz, R. L. 1993, *VizieR Online Data Catalog*, 6039, 0
 Lachaume, R., Dominik, C., Lanz, T., & Habing, H. J. 1999, *A&A*, 348, 897
 Lambert, D. L., & Reddy, B. E. 2004, *MNRAS*, 349, 757
 Lind, K., Asplund, M., & Barklem, P. S. 2009, *A&A*, 503, 541
 Luck, R. E., & Heiter, U. 2006, *AJ*, 131, 3069
 Mamajek, E. E., & Hillenbrand, L. A. 2008, *ApJ*, 687, 1264
 Meléndez, J., & Ramírez, I. 2007, *ApJ*, 669, L89
 Meléndez, J., Dodds-Eden, K., & Robles, J. A. 2006, *ApJ*, 641, L133
 Meléndez, J., Asplund, M., Gustafsson, B., & Yong, D. 2009, *ApJ*, 704, L66
 Meléndez, J., Ramírez, I., Casagrande, L., et al. 2010, *Ap&SS*, 328, 193
 Montalbán, J., & Schatzman, E. 2000, *A&A*, 354, 943
 Montalbán, J., & Rebolo, R. 2002, *A&A*, 386, 1039
 Nordström, B., Mayor, M., Andersen, J., et al. 2004, *A&A*, 418, 989
 Pasquini, L., Biazzo, K., Bonifacio, P., Randich, S., & Bedin, L. R. 2008, *A&A*, 489, 677
 Perryman, M. A. C., Lindegren, L., Kovalevsky, J., et al. 1997, *A&A*, 323, L49
 Pinsonneault, M. 1997, *ARA&A*, 35, 557
 Porto de Mello, G. F., Lyra, W., & Keller, G. R. 2008, *A&A*, 488, 653
 Ramírez, I., Meléndez, J., & Asplund, M. 2009, *A&A*, 508, L17
 Randich, S., Pallavicini, R., Meola, G., Stauffer, J. R., & Balachandran, S. C. 2001, *A&A*, 372, 862
 Reddy, B. E., Tomkin, J., Lambert, D. L., & Allende Prieto, C. 2003, *MNRAS*, 340, 304
 Rocha-Pinto, H. J., & Maciel, W. J. 1998, *MNRAS*, 298, 332
 Ryan, S. G. 2000, *MNRAS*, 316, L35
 Saffé, C., Gómez, M., & Chavero, C. 2005, *A&A*, 443, 609
 Sestito, P., & Randich, S. 2005, *A&A*, 442, 615
 Sestito, P., Randich, S., & Pallavicini, R. 2004, *A&A*, 426, 809
 Sneden, C. A. 1973, Ph.D. Thesis
 Soderblom, D. R. 1983, *ApJS*, 53, 1
 Soderblom, D. R., Fedele, S. B., Jones, B. F., Stauffer, J. R., & Prosser, C. F. 1993, *AJ*, 106, 1080
 Sousa, S. G., Santos, N. C., Mayor, M., et al. 2008, *A&A*, 487, 373
 Sousa, S. G., Fernandes, J., Israelian, G., & Santos, N. C. 2010, *A&A*, 512, L5
 Takeda, Y., & Tajitsu, A. 2009, *PASJ*, 61, 471
 Takeda, Y., Kawanomoto, S., Honda, S., Ando, H., & Sakurai, T. 2007, *A&A*, 468, 663
 Takeda, Y., Honda, S., Kawanomoto, S., Ando, H., & Sakurai, T. 2010, *A&A*, 515, A93
 Valenti, J. A., & Fischer, D. A. 2005, *ApJS*, 159, 141
 VandenBerg, D. A., Gustafsson, B., Edvardsson, B., Eriksson, K., & Ferguson, J. 2007, *ApJ*, 666, L105
 Vardavas, I. M. 2005, *MNRAS*, 363, L51
 Wright, J. T., Marcy, G. W., Butler, R. P., & Vogt, S. S. 2004, *ApJS*, 152, 261
 Xiong, D. R., & Deng, L. 2009, *MNRAS*, 395, 2013
 Yadav, R. K. S., Bedin, L. R., Piotto, G., et al. 2008, *A&A*, 484, 609
 Yi, S., Demarque, P., Kim, Y., et al. 2001, *ApJS*, 136, 417